Journal of Chromatography A, 1218 (2011) 5810–5818

Contents lists available at ScienceDirect

Journal of Chromatography A

journal homepage: www.elsevier.com/locate/chroma

Expanded separation technique for chlorophyll metabolites in Oriental tobacco leaf using non aqueous reversed phase chromatography

Naoyuki Ishida*

Tobacco Science Research Center, Japan Tobacco Inc., 6-2, Umegaoka, Aoba-ku, Yokohama, Kanagawa 227-8512, Japan

ARTICLE INFO

Article history:
Received 6 March 2011
Received in revised form 14 June 2011
Accepted 22 June 2011
Available online 30 June 2011

Keywords:
Chlorophyll
Chlorophyll metabolites
Oriental tobacco leaf
NARPC
DAD
APCI/MSD

ABSTRACT

An improved separation method for chlorophyll metabolites in Oriental tobacco leaf was developed. While Oriental leaf still gives the green color even after the curing process, little attention has been paid to the detailed composition of the remaining green pigments. This study aimed to identify the green pigments using non aqueous reversed phase chromatography (NARPC). To this end, liquid chromatograph (LC) equipped with a photo diode array detector (DAD) and an atmospheric pressure chemical ionization/mass spectrometer (APCI/MSD) was selected, because it is useful for detecting low polar non-volatile compounds giving green color such as pheophytin *a*. Identification was based on the wavelength spectrum, mass spectrum and retention time, comparing the analytes in Oriental leaf with the commercially available and synthesized components. Consequently, several chlorophyll metabolites such as hydroxypheophytin *a*, solanesyl pheophorbide *a* and solanesyl hydroxypheophorbide *a* were newly identified, in addition to typical green pigments such as chlorophyll *a* and pheophytin *a*. Chlorophyll metabolites bound to solanesol were considered the tobacco specific components. NARPC expanded the number of detectable low polar chlorophyll metabolites in Oriental tobacco leaf.

1. Introduction

Chlorophylls play the most essential role in various plant activities. They are formed in the thylakoid lumen of chloroplast and are correlated with photosynthesis reactions that eventually convert carbon dioxide and water to oxygen and carbohydrate [1]. Much attention has been paid to chlorophylls due to not only scientific interests in dynamic photosynthesis, but also future applications based on mechanistic considerations.

The crucial and various properties of chlorophylls are mainly derived from their complex structures [2]. They are comprised of a porphyrin, a magnesium ion in the center and the long diterpenoid alcohol called phytol (Fig. 1). The most specific structure observed on chlorophylls is a long and widespread <pi> electron conjugated system delocalized over four pyrrole rings. This system has two pieces of large absorbance in the range of optical wavelength and explains why chlorophylls provide plant leaves with specific colors and the energy transfer to subsequent photosynthetic processes to form carbon dioxide [1]. Additionally, from their mutual differences in structure, chlorophylls are classified into several types, such as chlorophyll *a*, *b*, *c*1, *c*2, *d* [3] and *f* [4]. The different absorbance between chlorophyll *a* and *b* originates from the terminal group at the R_1 position (Fig. 1) [1,5]. Since the aldehyde group of R_1 of chlorophyll *b* is an electron-withdrawing group which is thought to affect the <pi> electron conjugated system more than methyl group of chlorophyll *a*, chlorophyll *b* that has the absorbance (453, 643 nm [6]) gives a different absorbance from chlorophyll *a* that has the absorbance (430, 662 nm [6]).

Chlorophyllide *a*, pheophytin *a* and pheophorbide *a* (Fig. 1) are also known for their degraded forms of chlorophylls [7–11] which are defined as chlorophyll metabolites in this document. Since the maximum absorption wavelength of chlorophyllide *a* (428, 662 nm [6]) is almost the same as chlorophyll *a*, chlorophyllide *a* is thought to give the similar green color to chlorophyll *a* even if the phytyl group is eliminated from the R_2 position [5]. On the other hand, pheophytin *a* not including a magnesium ion, but holding a phytyl group, is not expected to give a similar green color to chlorophyllide *a*. Actually, the previous data regarding absorption wavelength (408, 667 nm [6]) also indicated it. This difference between chlorophyllide *a* and pheophytin *a* is considered coming from a magnesium ion in the center greatly affecting the <pi> electron conjugated system more than the electronically inactive side chain groups [5]. Nevertheless, the remaining <pi> electron conjugated system may still give the green color to pheophytin *a*. A similar prediction could be made for pheophorbide *a*, because it still retains the conjugated system and thereby gives almost the same absorption wavelength (408, 665 nm [6]) as pheophytin *a*.

The green color of plant leaf notably diminishes owing to the degradation of chlorophylls. The degradation begins with the

* Tel.: +81 45 345 5170; fax: +81 45 973 6781.
E-mail address: naoyuki.ishida@jt.com

0021-9673/$ – see front matter © 2011 Elsevier B.V. All rights reserved.
doi:10.1016/j.chroma.2011.06.082

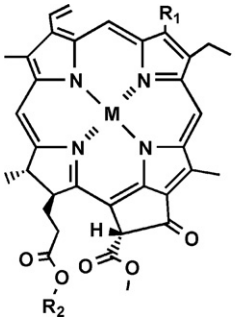

	R_1	R_2	M	Max abs. (nm)	
Chlorophyll *a*	CH_3	Phytyl	Mg	430, 662	Chlorophylls
Chlorophyll *b*	CHO	Phytyl	Mg	453, 643	
Pheophytin *a*	CH_3	Phytyl	2H	408, 667	Chlorophyll metabolites
Chlorophyllide *a*	CH_3	H	Mg	428, 662	
Pheophorbide *a*	CH_3	H	2H	408, 665	

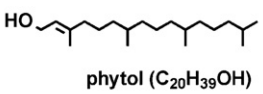

phytol ($C_{20}H_{39}OH$)

Fig. 1. Structures of chlorophylls and chlorophyll metabolites. Maximum wavelength absorptions in the table were from the previous report [6].

termination of plant cells that naturally occurs just after harvesting or leaf shedding. Since carotenoid is degraded more slowly than chlorophylls, autumnal color emerges in fall-time leaves more vividly than fresh leaves. Chlorophylls in tobacco leaves such as flue-cured Virginia and burley also decrease under the curing process, a drying process for usage [12–14]. Accordingly, tobacco leaf after the curing process does not give a green color.

However, Oriental leaf, a type of tobacco leaf that is mainly cultivated in Turkey and Greece, still remains green even after the sun air curing process, a drying process exposed to sun light different from flue-cured Virginia (usually dried with artificial heat for 5–7 days) and burley (usually dried at ambient temperature for longer time than flue-cured Virginia). Flue-cured Virginia and Oriental are known for the larger amount of reducing sugar and the smaller amount of protein than burley. The detailed different compositions of them partly due to their different curing processes are summarized in the previous report [14]. In addition, while burley leaf dried in darkness did not include chlorophylls, 0.021 mg/g of chlorophyll *a* was reported in burley dried under light even after 90 days [13]. Although the remaining chlorophylls were considered to be caused by high temperature derived from light, the cause and composition of green pigments still has remained unclear.

Green pigments other than remaining chlorophylls in Oriental leaf were considered chlorophyll metabolites such as pheophytin *a*, chlorophyllide *a* or pheophorbide *a*, not only because chlorophylls decrease under the curing process and change into chlorophyll metabolites [14], but also because pheophytin *a* has already been reported as a green pigment included in green tea leaves that require multiple steps for drying [15]. For this reason, chlorophyll metabolites were the target components that should be analyzed first. The clarification of chlorophyll metabolites was considered helpful for understanding the specific character of Oriental and the chemical change during the curing process. These basic investigations were expected to become the first step for it. Considering these backgrounds, the objective of this research is to develop an appropriate analytical method and subsequently clarify these targeted chlorophyll metabolites.

The instrument for the detection and identification of chlorophyll metabolites was determined dependent on their following three structural features: (1) high molecular weight over 800, (2) low polarity and (3) optical wavelength absorption. Therefore, liquid chromatograph (LC) equipped with a photo diode array detector (DAD) for the detection of green color and an atmospheric pressure chemical ionization/mass spectrometric detector (APCI/MSD) for the ionization of molecules with low polarity and high molecular weight was selected as the instrument for the identification of chlorophyll metabolites in Oriental leaf.

In the first part of this research, the chromatographic condition for the separation of chlorophyll metabolites is discussed. The unknown chlorophyll metabolites are identified by comparing analytes with commercially available and synthesized components based on the retention time, absorption wavelength and mass spectrum. The origin and biosynthetic pathway of identified chlorophyll metabolites is mentioned in the last section.

2. Experimental

2.1. Materials

Tobacco leaves (Flue-cured Virginia from Brazil, Oriental from Turkey and Dark air-cured leaf from Japan) were stored in a warehouse of Japan Tobacco Inc. and used for the analysis of chlorophyll metabolites. Solvents were purchased from Wako Pure Chemical Industries, Ltd. (Tokyo, Japan). Chlorophyll *a*, chlorophyll *b*, pheophytin *a* and pheophytin *b* were purchased from Wako Pure Chemical Industries, Ltd. (Tokyo, Japan) for identification. Pheophytin *a* was also used for the synthesis of hydroxypheophytin *a*. The synthesis of chlorophyll metabolites for identification was accomplished by all of the following reagents. Solanesol, 1,8-diazabicyclo[5.4.0]undec-7-ene (DBU), (*1R*)-(+)-(10-camphorsulfonyl)oxaziridine ((+)-CSOAI), and di-*tert*-butyl dicarbonate ($(Boc)_2O$) were purchased from Tokyo Chemical Industry Co., Ltd. (Tokyo, Japan). Pheophorbide *a*, dehydrated pyridine (Py), and 4-dimethylaminopyridine (DMAP) were from Wako Pure Chemical Industries, Ltd. (Tokyo, Japan). Dehydrated tetrahydrofuran (THF) as the solvent for synthesis was purchased from Kanto Chemical Co., Inc. (Tokyo, Japan).

2.2. Sample preparation

Approximately 100 g of tobacco leaves were pulverized in a 1-mm mesh using a CYCLOTEC 1093 Sample mill (FOSS TECATOR Inc., Höganäs, Sweden). The 10-g pulverized sample was put into a 300 mL Erlenmeyer flask, extracted with acetone assisted by ultrasonic equipment UT206 (Sharp Manufacturing Systems Corporation, Osaka, Japan) and filtrated with a filter paper #1 6 μm (Tokyo Roshi Kaisha Ltd., Tokyo, Japan). The total volume of collected acetone solution was adjusted to 250 mL by volumetric flask and filtrated with Millex-LG with a pore size of 0.20 μm (Millipore Corporation, Bedford, MA, USA) to remove the insoluble components in acetone solution. This solution was subsequently injected into the analytical instrument.

2.3. Instrument condition

2.3.1. Reversed phase chromatography for identification of chlorophyll metabolites

HPLC analysis was performed using an Agilent 1200 HPLC system equipped with DAD G1315C (Agilent Tech., CA, USA) incorporating 6 mm flow cell G1315-60015 (Agilent Tech., CA, USA). A LiChrospher RP18 column (250 mm × 4.6 mm I.D., 5 μm, Supelco Inc., PA, USA) was used under the following conditions. Mobile

phase A (aqueous 1 M ammonium acetate/MeOH = 1/4), mobile phase B (acetone/MeOH = 1/4); flow rate 1.0 mL/min; gradient condition A 100% at 0 min, A 0% at 15 min with linear gradient and A 0% (B 100%) holding until 60 min; injection volume 50 μL; column temperature 25 °C. Measurement of wavelength absorption using DAD was configured in the range of 190–800 nm.

2.3.2. Non aqueous reversed phase chromatography for identification of chlorophyll metabolites

HPLC analysis was performed using an Agilent 1200 HPLC system equipped with DAD G1315 C and 6130 APCI/MSD (Agilent Tech., CA, USA) incorporating 6 mm flow cell G1315-60015 (Agilent Tech., CA, USA). An Excelpak SIL-C18/5 C column (250 mm × 4.6 mm I.D., 5 μm, Yokogawa Analytical Systems, Japan (currently available from Agilent Tech.)) was used under the following conditions. Mobile phase A (acetonitrile), mobile phase B (acetone); flow rate 1.0 mL/min; gradient condition A 100% at 0 min, A 30% at 10 min, A 20% at 30 min, A 0% at 40 min, and A 0% (B 100%) holding until 55 min; injection volume 50 μL; column temperature 25 °C. Measurements of wavelength absorption using DAD were configured at 190–800 nm for identification. APCI/MSD was used under the following conditions: capillary voltage 4000 V; Corona current 10 μA; drying gas flow 5 mL/min; drying gas temperature 350 °C; fragmentor voltage 200 V; nebulizer pressure 60 psi; vaporizer temperature 500 °C; 100–1850 *m/z* on scan mode to detect large molecular weight. Mass spectrum for further certification was acquired on the selected ion monitoring mode detecting only the specific fragments from each component (see Table 2). The flow rate of this analysis was split into 3/13 (about 0.23 mL/min) just before entering the sprayer of the APCI interface.

2.4. Preparation of chlorophyll metabolites

2.4.1. Solanesyl pheophorbide a

The synthesis started by dissolving pheophorbide *a* (*a*/*a*′ = 85.5/14.5) in dehydrated THF in a two-necked flask filled with argon gas at −42 °C. Then, dehydrated Py was injected dropwise through a syringe, and a catalytic amount of DMAP was added. The resulting solution was stirred for more than 10 min. Afterward, $(Boc)_2O$ in THF was added dropwise to the mixture. Ten minutes later, solanesol was added to the mixture. After the solution was stirred for 4 h, it was quenched by 0.05 M aqueous hydrochloride, extracted by *n*-hexane 3 times, washed with saturated sodium chloride water and dried by dehydrated sodium sulfate. The resulting residue was purified by PLC 1.138959 (MERCK KGaA Inc., Darmstadt, Germany) (SiO_2, hexane/AcOEt = 5/5) to give solanesyl pheophorbide *a* (*a*/*a*′ = 95.3/4.7 determined by HPLC) as the green component. All procedures were performed under the condition shielded from light based on a previous report [16].

2.4.2. Hydroxypheophytin a and solanesyl hydroxypheophorbide a

The synthesis started by dissolving pheophytin *a* (*a*/*a*′ = 84.5/15.5) in THF, and adding DBU dropwise. Then, the mixture was stirred at −42 °C for 10 min. (+)-CSOAI in THF was added to the mixture dropwise and stirred for more than 4 h. The resultant mixture was handles in the same way as Section 2.4.1. The remaining residue was purified by PLC 1.138959 (MERCK KGaA Inc., Darmstadt, Germany) (SiO_2, hexane/AcOEt = 7/3) to give hydroxypheophytin *a* (*a*/*a*′ = 38.4/61.6 by HPLC) as the dark green component. All procedures were conducted under the condition shielded from light based on a previous report [17]. The synthesis of solanesyl hydroxypheophorbide *a* starting from solanesyl pheophorbide *a* was based on the same procedure as hydroxypheophytin *a*. This yielded the dark green component (*a*/*a*′ = 32.7/67.3 by HPLC).

3. Results and discussion

3.1. Improvement of separation

Since the separation of chlorophylls and chlorophyll metabolites using reversed phase chromatography (RP) has already been accomplished [6,18–20], the initial part of our research started from the comparison between flue-cured Virginia and Oriental using RP condition [18]. Fig. 2 shows the RP chromatograms by LC/DAD configured at 660 nm. Although much more chlorophyll *a*, pheophytin *a* and pheophorbide *a* were included in Oriental leaf than in flue-cured Virginia, Chlorophyllide *a* was not detected in both of them. Given the large peak of pheophorbide *a* and small peak of chlorophyll *a*, it was possible that chlorophyll metabolites among green pigments were the main components in Oriental leaf. Interestingly, the unknown peaks around and behind pheophytin *a* were also detected on the chromatogram. However, they were flattened or overlapped by the other component. Additionally, this method could not be applied to a mass spectrometer due to the high concentrate of aqueous 1 M ammonium acetate in eluent. Since further

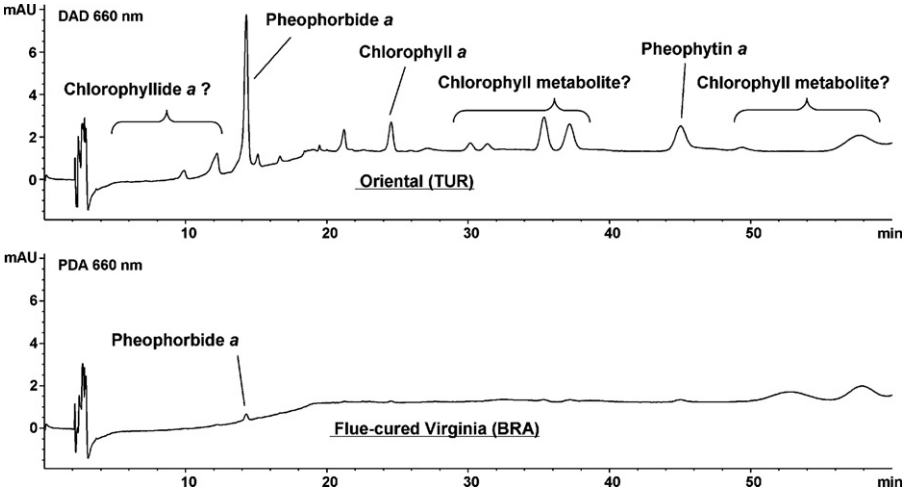

Fig. 2. RP chromatograms of flue-cured Virginia and Oriental leaf which were performed by a typical method using LC/DAD configured at 660 nm. The analytical condition is described in Section 2.3.1. Abbreviations of growing districts are as follows: BRA, Brazil; TUR, Turkey.

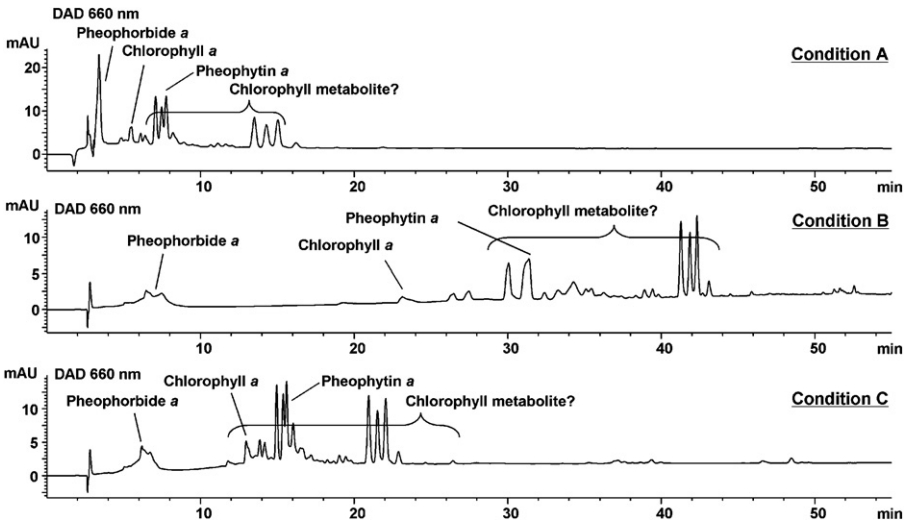

Fig. 3. Chromatograms of Oriental using LC/DAD under various NARPC conditions. Mobile phase A (acetonitrile), Mobile phase B (acetone), Condition A [26]: A 30% at 0 min, A 20% at 35 min with linear gradient, A 20% until 55 min. Condition B: A 100% at 0 min, A 0% at 50 min with linear gradient, A 0% until 55 min. Condition C: A 100% at 0 min, A 30% at 10 min with linear gradient, A 0% at 55 min with linear gradient. The other instrumental conditions are the same described in Section 2.3.2.

identification of the unknown components was difficult, another separation technique was explored.

The insufficient separation was considered to result from the eluent condition including water and buffer salt. Such polar eluent was unlikely to separate low polar chlorophyll metabolites like pheophytin *a*. For this reason, NARPC that utilizes lower polar eluent than semi-aqueous methanol and acetonitrile [21] was selected due to its known capability of separating low polar components like triacylglycerol and steroid [22–26]. Since pheophytin *a* also possesses a low polar structure, NARPC was expected to become the powerful tool to separate the unknown low polar chlorophyll metabolites. In addition, NARPC without buffer salt made it possible to use MSD with APCI interface which is known for being able to ionize low polar components.

The development of method using only acetone and acetonitrile as eluent began with the use of previously reported condition [26] (condition A in Fig. 3). Although it could separate the chlorophyll metabolites in 20 min, the mass spectrum was not usable to identify them due to the existence of the other components (data not shown). Since the concentrate of acetone was considered effective for elution of low polar chlorophyll metabolites, the initial concentrate of acetonitrile was increased up to 100%, and then acetone was added with a linear gradient up to 100% (condition B in Fig. 3). Although it consequently delayed the retention times of chlorophyll metabolites, it was hard to detect chlorophylls (23 min), gave the overlapped peaks (31 min) and took long time for elution. Thus, the condition C (Fig. 3), in which the initial linear gradient of acetone was increased more than condition B and then maintained in the same analytical time, was investigated. It showed the better separation of chlorophyll metabolites in addition to the mass chromatograms. In the end, the condition shown in Fig. 4 was selected.

The chromatograms using the NARPC technique with acetone and LC/DAD distinctly showed the various types of chlorophyll metabolites around and behind pheophytin *a* (Fig. 4). As mentioned above, the green pigments in flue-cured Virginia were not observed. Although only pheophorbide *a* with the free carboxylic acid group gave a broadened peak possibly due to the lack of buffer salt, the peak shapes of the other components were drastically improved. These unknown peaks also showed two pieces of large absorbance on wavelength spectrum derived from <pi> electron conjugated

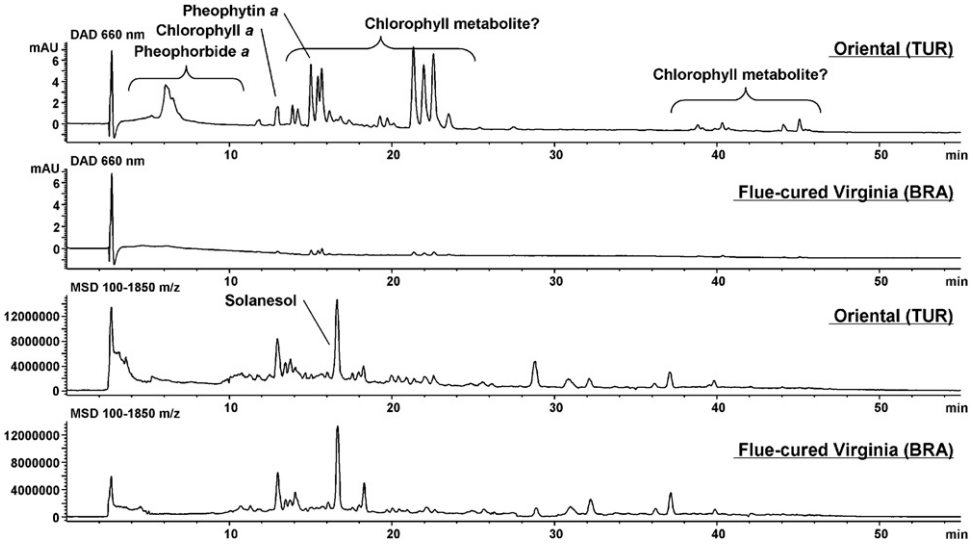

Fig. 4. NARPC chromatograms of flue-cured Virginia and Oriental leaf using LC/DAD configured at 660 nm and APCI/MSD scan mode. The analytical condition is described in Section 2.3.2.

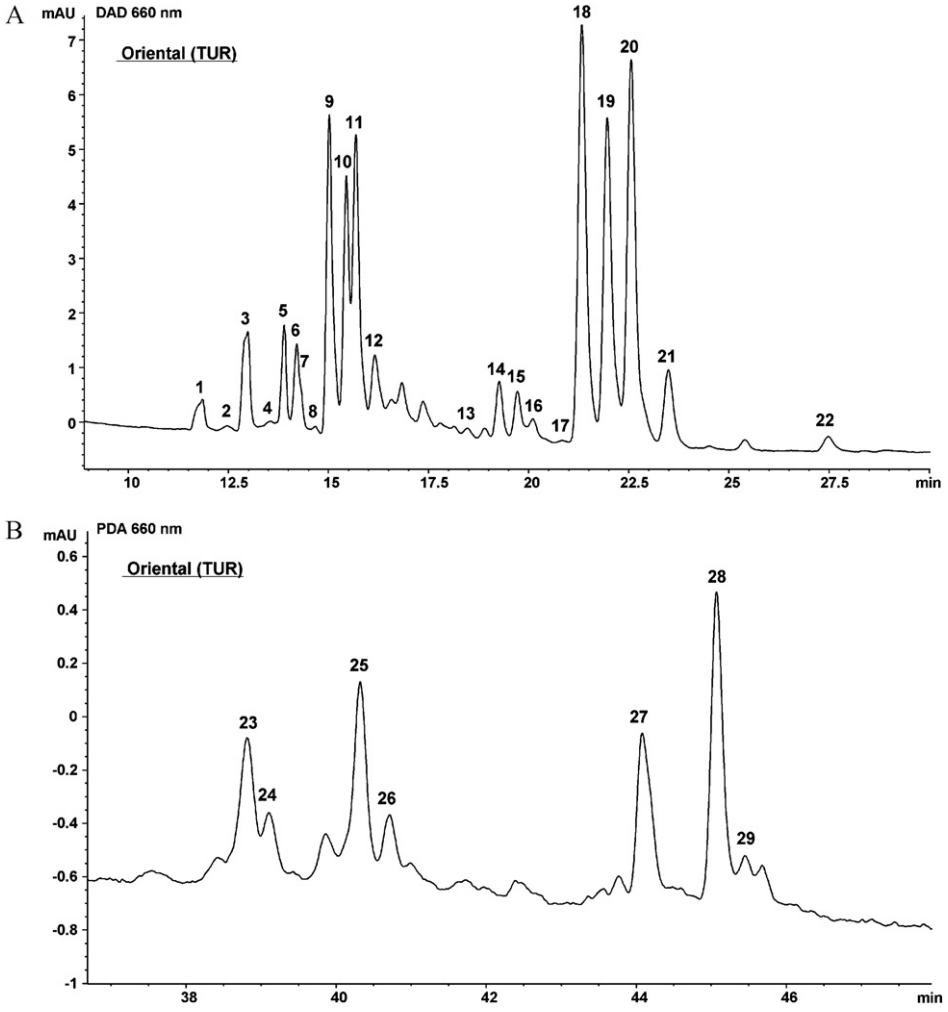

Fig. 5. (A) Extended chromatogram of Fig. 4 on the left. (B) Extended chromatogram of Fig. 4 on the right.

structure. They were thereby considered the chlorophyll metabolites that should be identified. The previous report using RP could also give the separation of lower polar chlorophyll metabolites than pheophytin *a* within about 110 min [20]. The developed method using acetone fortunately provided the same performance for such components in Oriental within 60 min. If the components for analysis are limited to the main ones before 30 min on the chromatogram, the further shortened analytical time will be available.

This method also provided the chromatograms by APCI/MSD (Fig. 4) different from the chromatograms by DAD. They did not show the large difference regarding the chlorophyll metabolites. However, the mass spectrums from each component were of great help for the identification of chlorophyll metabolites as in the following sections. Additionally, this method might make it possible to detect the other low polar components in tobacco leaf like triacylglycerol and steroid at the same run and be applicable for the components in the other dried plant like tea.

3.2. Identification of chlorophyll metabolites

The specific wavelength spectrum observed in chlorophyll and chlorophyll metabolites was of great assistance in determining which peak is likely to be a chlorophyll metabolite. Mass spectrum enabled us to predict the molecular weight and the structure of chlorophyll metabolites. The predicted components were synthesized in order to determine whether their retention time is identical to the analyte and they give the same spectrometric data. In this way, the identification was basically conducted through comparing the analytes in Oriental leaf with the commercially available and synthesized components. Some unknown chlorophyll metabolites were determined by previous reports and structural data obtained from our analysis.

All the identified chlorophyll metabolites are shown in Figs. 5A and B and 6 with the detailed structure of chlorophylls and chlorophyll metabolites. All spectrometric date is summarized in Tables 1 and 2. Chlorophyll *a* (**3**), (*a*′ = **4**), chlorophyll *b* (**1**), (*b*′ = **2**), pheophytin *a* (**11**), (*a*′ = **12**) and pheophytin *b* (7), (*b*′ = **8**) were easily identified by commercially available standards. The retention times of these components in Oriental leaf coincided with the standard components. The prime attached to the component names such as chlorophyll *a*′ indicates the diastereomer related to the chiral center bound to the R_3 and R_4 group. The components without prime commonly eluted out before the components with prime. Whenever a reversed phase chromatography was applied, the same elution order was seen without regard to the intricate structure of chlorophyll and chlorophyll metabolites. This tendency largely contributed to the identification of unknown chlorophyll metabolites.

Some other types of chlorophyll metabolites were identified with the wavelength spectrum, mass spectrum and retention time of synthesized components. Fig. 7 shows the comparison of the retention time between the unknown peaks in Oriental and the synthesized ones; hydroxypheophytin *a* (**9**), (*a*′ = **10**), solanesyl pheophorbide *a* (**20**), (*a*′ = **21**) and solanesyl hydroxypheophorbide

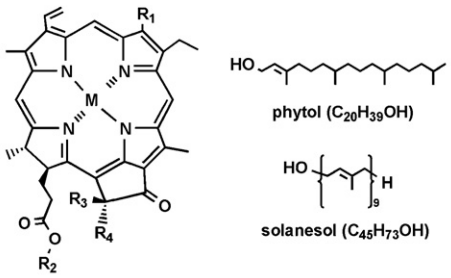

number	retention (min)	assignment	M	R_1	R_2	R_3	R_4
1	12.03	Chlorophyll *b*	Mg	CHO	Phytyl	H	$COOCH_3$
2	12.60	Chlorophyll *b'*	Mg	CHO	Phytyl	$COOCH_3$	H
3	13.14	Chlorophyll *a*	Mg	CH_3	Phytyl	H	$COOCH_3$
4	13.65	Chlorophyll *a'*	Mg	CH_3	Phytyl	$COOCH_3$	H
5	13.84	Hydroxypheophytin *b*	2H	CHO	Phytyl	OH	$COOCH_3$
6	14.15	Hydroxypheophytin *b'*	2H	CHO	Phytyl	$COOCH_3$	OH
7	14.30	Pheophytin *b*	2H	CHO	Phytyl	H	$COOCH_3$
8	14.57	Pheophytin *b'*	2H	CHO	Phytyl	$COOCH_3$	H
9	14.93	Hydroxypheophytin *a*	2H	CH_3	Phytyl	OH	$COOCH_3$
10	15.36	Hydroxypheophytin *a'*	2H	CH_3	Phytyl	$COOCH_3$	OH
11	15.58	Pheophytin *a*	2H	CH_3	Phytyl	H	$COOCH_3$
12	16.04	Pheophytin *a'*	2H	CH_3	Phytyl	$COOCH_3$	H
13	18.31	Pyropheophytin *a*	2H	CH_3	Phytyl	H	H
14	19.18	Solanesyl hydroxypheophorbide *b*	2H	CHO	Solanesyl	OH	$COOCH_3$
15	19.63	Solanesyl hydroxypheophorbide *b'*	2H	CHO	Solanesyl	$COOCH_3$	OH
16	20.01	Solanesyl pheophorbide *b*	2H	CHO	Solanesyl	H	$COOCH_3$
17	20.75	Solanesyl pheophorbide *b'*	2H	CHO	Solanesyl	$COOCH_3$	H
18	21.19	Solanesyl hydroxypheophorbide *a*	2H	CH_3	Solanesyl	OH	$COOCH_3$
19	21.82	Solanesyl hydroxypheophorbide *a'*	2H	CH_3	Solanesyl	$COOCH_3$	OH
20	22.40	Solanesyl pheophorbide *a*	2H	CH_3	Solanesyl	H	$COOCH_3$
21	23.31	Solanesyl pheophorbide *a'*	2H	CH_3	Solanesyl	COOCH3	H
22	27.26	Solanesyl pyropheophorbide *a*	2H	CH_3	Solanesyl	H	H
23	38.63	Solanesyl hydroxypheophytin *a*	2H	CH_3	Phytyl	OH	$COOC_{45}H_{73}$
24	38.93	Solanesyl hydroxypheophytin *a'*	2H	CH_3	Phytyl	$COOC_{45}H_{73}$	OH
25	40.16	Solanesyl pheophytin *a*	2H	CH_3	Phytyl	H	$COOC_{45}H_{73}$
26	40.54	Solanesyl pheophytin *a'*	2H	CH_3	Phytyl	$COOC_{45}H_{73}$	H
27	43.96	Disolanesyl hydroxypheophorbide *a*/*a'*	2H	CH_3	Solanesyl	OH	$COOC_{45}H_{73}$
28	44.92	Disolanesyl pheophorbide *a*	2H	CH_3	Solanesyl	H	$COOC_{45}H_{73}$
29	45.30	Disolanesyl pheophorbide *a'*	2H	CH_3	Solanesyl	$COOC_{45}H_{73}$	H

Fig. 6. Assignment of identified chlorophylls and chlorophyll metabolites. The retention times were determined by DAD configured at 660 nm.

a (**18**), (*a'* = **19**). Hydroxypheophytin *a* is a chlorophyll metabolite that includes a hydroxy group at the carbon atom with a methoxy carbony group of pheophytin *a* and has already been reported in plants other than tobacco leaf. Solanesol is a long terpenoid alcohol and was first isolated from tobacco leaf [27]. The chlorophyll metabolites including the solanesyl group instead of phytol were considered representative among the chlorophyll metabolites in Oriental. These synthesized components eluted out from the column at the same retention time on the chromatogram as the corresponding components in Oriental (Fig. 7). They also

Table 1
Maximum absorption of chlorophylls and chlorophyll metabolites on wavelength spectrum. The analytical condition is described in Section 2.3.2. "Standard" in the identification column means that the identification was performed by commercially available or synthesized components. "DAD, MSD" means that they were determined by their analytical data. The marker (*) indicates synthesized components. Reported maximum absorption was based on a previous report [19].

Number	λ_{max} (analyte)	λ_{max} (available or synthesized standard)	λ_{max} (reported)	Identification
1	456, 594, 644	454, 596, 644	462, 600, 648	Standard
2	456, 648	454, 596, 644	462, 600, 648	Standard
3	430, 618, 662	430, 616, 660	430, 618, 664	Standard
4	664	430, 618, 662	430, 618, 664	Standard
5	432, 526, 554, 596, 652		434, 522, 598, 652	DAD, MSD
6	434, 526, 554, 596, 652		436, 528, 600, 652	DAD, MSD
7	434, 526, 550, 596, 652	434, 524, 598, 652	436, 528, 598, 652	Standard
8	434, 652	434, 526, 552, 596, 652	436, 524, 600, 656	Standard
9	406, 502, 530, 608, 664	408, 502, 530, 608, 664	406, 502, 532, 610, 666	*Standard
10	410, 502, 532, 608, 666	410, 502, 532, 608, 666	408, 504, 534, 610, 666	*Standard
11	408, 504, 534, 608, 664	408, 504, 534, 608, 664	408, 506, 536, 608, 666	Standard
12	408, 502, 534, 608, 666	408, 504, 536, 608, 666	408, 506, 536, 610, 666	Standard
13	410, 664		410, 508, 538, 610, 666	DAD, MSD
14	432, 522, 600, 652			DAD, MSD
15	434, 522, 600, 652			DAD, MSD
16	434, 520, 596, 652			DAD, MSD
17	436, 652			DAD, MSD
18	406, 502, 530, 610, 666	404, 502, 530, 608, 666		*Standard
19	410, 502, 532, 610, 666	410, 502, 532, 610, 666		*Standard
20	408, 504, 534, 606, 664	408, 504, 534, 610, 664		*Standard
21	410, 504, 536, 606, 666	408, 504, 534, 610, 666		*Standard
22	410, 664			DAD, MSD
23	410, 506, 534, 612, 666			DAD, MSD
24	408, 610, 666			DAD, MSD
25	410, 504, 534, 604, 666			DAD, MSD
26	402, 668			DAD, MSD
27	408, 500, 532, 610, 666			DAD, MSD
28	408, 504, 536, 608, 666			DAD, MSD
29	406, 668			DAD, MSD

Table 2
Specific fragments observed in chlorophylls and chlorophyll metabolites. The analytical condition is described in Section 2.3.2. The numbers in parentheses indicate the relative intensity compared to base peak on each mass spectrum. The retention times are slightly different from those in Table 1 due to a delay between the DAD detector and mass spectrometer.

Number	Retention (min)	$[M+H^+]$ (analyte)	$[M+H^+]$ (available or synthesized standard)
1	12.04	907.6(100), 629.2(44.5)	907.6(100), 629.2(65.3)
2	–	907.6(100), 629.2(N.D.)	907.6(100), 629.2(48.2)
3	13.24	893.5(100), 615.2(59.6)	893.5(100), 615.2(51.9)
4	–	893.5(100), 615.2(N.D.)	893.5(86.8), 615.2(100)
5	13.96	901.5(85.6), 883.5(65.9), 623.4(45.2), 605.3(100)	
6	14.27	901.5(100), 883.5(13.4), 623.4(53.6), 605.3(51.8)	
7	14.37	885.5(100), 607.4(87.7)	885.5(100), 607.4(86.7)
8	14.74	885.5(100), 607.4(N.D.)	885.5(100), 607.4(94.6)
9	15.06	887.5(86.2), 869.5(100), 609.4(13.6), 591.2(42.8)	887.5(96.3), 869.5(100), 609.4(23.8), 591.2(45.5)
10	15.48	887.5(100), 869.5(34.3), 609.4(52.9), 591.2(41.3)	887.5(100), 869.5(37.2), 609.4(41.0), 591.2(41.8)
11	15.71	871.5(100), 593.3(82.9)	871.5(100), 593.3(81.0)
12	16.15	871.5(100), 593.3(48.3)	871.5(100), 593.3(59.4)
13	18.46	813.8(100), 535.6(6.0)	
14	19.33	1235.7(100), 1217.7(40.9), 623.3(53.3), 605.3(49.5)	
15	19.75	1235.7(100), 1217.7(6.9), 623.3(94.0), 605.3(37.7)	
16	20.14	1219.7(100), 607.4(53.6)	
17	20.88	1219.7(100), 607.4(78.6)	
18	21.33	1221.7(100), 1203.7(67.7), 609.3(24.5), 591.2(28.7)	1221.7(100), 1203.7(50.4), 609.3(21.8), 591.2(20.7)
19	21.95	1221.7(100), 1203.7(26.8), 609.3(43.3), 591.2(29.3)	1221.7(100), 1203.7(24.9), 609.3(46.0), 591.2(27.6)
20	22.54	1205.7(100), 1173.7(13.4), 593.3(47.9)	1205.7(100), 1173.7(8.5), 593.3(46.2)
21	23.43	1205.7(100), 1173.7(6.4), 593.3(48.4)	1205.7(100), 1173.7(3.7), 593.3(45.9)
22	27.40	1147.8(100), 535.6(7.1)	
23	38.79	1486.1(100), 1468.0(98.0), 1207.6(24.5)	
24	39.05	1486.1(100), 1468.0(21.5), 1207.6(18.0)	
25	40.29	1470.1(53.7), 857.4(42.4), 839.6(34.1), 813.6(100)	
26	40.68	1470.1(66.0), 857.4(55.0), 839.6(23.0), 813.6(100)	
27	44.10	1820.3(81.3), 1207.8(100), 1187.8(0.52), 1163.8(35.3)	
28	45.06	1804.4(14.7), 1191.8(19.9), 1173.8(25.6), 1147.8(100)	
29	45.42	1804.4(31.3), 1191.8(34.5), 1173.8(20.5), 1147.8(100)	

showed the same wavelength spectrum and mass spectrum as the analytes in Oreintal (Tables 1 and 2). In the case of solanesyl pheophorbide *a*/*a*′ (**20**/**21**) (Fig. 8), the analyte gave the two large and small three pieces of absorbance similar to pheophytin *a*. The synthesized one also showed the same spectrum. Mass spectrum of the analyte exhibited a similar pattern to the synthesized one, including the removal of methanol (CH_3OH), solanadiene ($C_{45}H_{72}$) and the solanesyl acetate group ($CH_3COOC_{45}H_{73}$) through fragmentation. A report that referred to the removal of methanol (CH_3OH), phytadien ($C_{20}H_{38}$) and phytyl acetate ($CH_3COOC_{20}H_{39}$) [18,28] supported that it was solanesyl pheophorbide *a*/*a*′ (**20**/**21**). Hydroxypheophytin *a*/*a*′ (**9**/**10**) and solanesyl hydroxypheophorbide *a* (**18**/**19**) were identified in the same procedures. After some of the unknown chlorophyll metabolites were identified by the standard components, the unknown peaks on the RP chromatograms (Fig. 2) were confirmed by the commercially available and synthesized components. Hydroxypheophytin *a* (**9**), *a*′ (**10**) and pheophytin *b* (**7**) were identified on the DAD chromatogram (**9** at 35 min, **10** and **7** at 37 min in Fig. 2). On the other hand, it was difficult to detect solanesylated chlorophyll metabolites (**18**–**21**) even if the synthesized components were used for identification. This result indicated that the use of NARPC for chlorophyll metabolites is effective for the lower polar chlorophyll metabolites than traditional chlorophylls.

The remaining chlorophyll metabolites such as hydroxypheophytin *b*/*b*′ (**5**/**6**), solanesyl pheophorbide *b*/*b*′ (**16**/**17**), solanesyl hydroxypheophorbide *b*/*b*′ (**14**/**15**), pyropheophytin *a* (**13**) and solanesyl pyropheophorbide *a* (**22**) were determined by the wavelength spectrum, mass spectrum and elution orders based on previous reports [6,18–20]. The chlorophyll metabolites of *b* types such as pheophytin *b* including the aldehyde group on the side

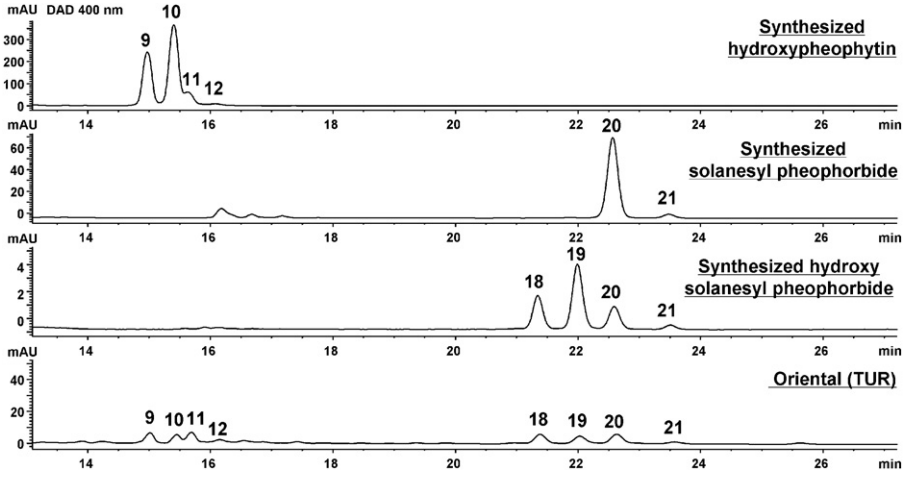

Fig. 7. Chromatograms comparing synthesized chlorophyll metabolites with the analytes in Oriental leaf by DAD configured at 400 nm. The analytical condition is described in Section 2.3.2.

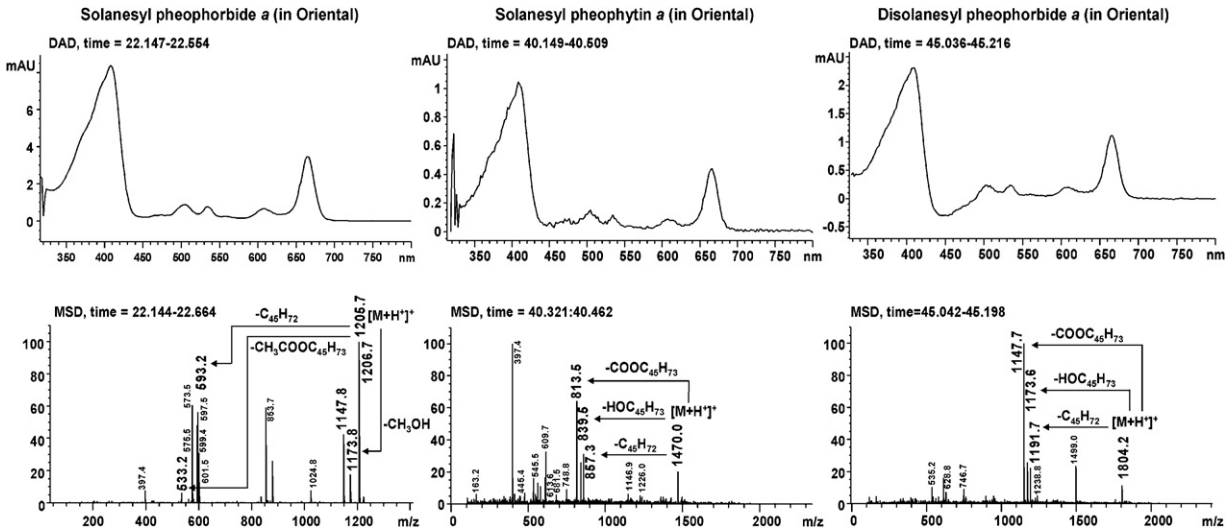

Fig. 8. The wavelength spectrums and mass spectrums of solanesyl pheophorbide *a*, solanesyl pheophytin *a* and disolanesyl pheophorbide *a* in Oriental leaf. The analytical condition is described in Section 2.3.2.

chain eluted out faster than *a* types with methyl at the same position. Thus, the retention times of type *b* components were predicted only if the corresponding components of type *a* were firmly identified. Additionally, the wavelength spectrums specific to type *b* were useful for determination because they gave two large wavelength absorptions around 430 and 650 nm differing from type *a*. Moreover, the precursor ion on the mass spectrum derived from type *b* was of great assistance in the determination because it was the precursor ion added to type *a* by 14 *m*/*z* due to the aldehyde group instead of the methyl group.

The chromatogram in the latter part also included several unknown chlorophyll metabolites (Fig. 5B). The wavelength spectrums and mass spectrums of solanesyl pheophytin *a* (**25**) and disolanesyl pheophorbide *a* (**28**) are shown in Fig. 8. Both of the components strongly indicated that they have the <pi> electron conjugated system giving two pieces of large absorbance. Their mass spectrums included the same fragment ion as the precursor ion of pyropheophytin *a* (813.5 *m*/*z*) (**13**) and solanesyl pyropheophorbide *a* (1147.7 *m*/*z*) (**22**). The fact that solanesyl pheophorbide *a* (**20**) was fragmented into solanesyl pyropheophorbide *a* (1147.8 *m*/*z*) (**22**) due to the elimination of methyl formate ($COOCH_3$) (Fig. 8) indicated that the elimination of solanesyl formate ($COOC_{45}H_{73}$) also occurred in these components. Additionally, their fragmentations included the elimination of solanadiene ($C_{45}H_{72}$) and solanesol ($C_{45}H_{73}OH$). Considering these chemical data, the most feasible components were solanesyl pheophytin *a* (**25**) and disolanesyl pheophorbide *a* (**28**). Similarly, hydroxylated forms such as solanesyl hydroxypheophytin *a* (**23**) and disolanesyl hydroxypheophorbide *a*/*a*′ (**27**) were determined, though components (**27**) were not separated into *a* and *a*′ type. Although the amounts of them were much smaller than the other chlorophyll metabolites, the use of NARPC made it possible to determine such components in Oriental leaf.

The wavelength spectrums of each component showed the two large absorptions (Tables 1 and 2). The maximum absorptions on some components were almost identical to the commercially available and synthesized components. On the other hand, the scan range of the mass spectrometer was too wide (e.g. 100–1850 *m*/*z*) to have sufficient ion intensity and fragmentation stabilization. For this reason, it was difficult to compare the fragmentation patterns between the analyte and standard component. Therefore, after each mass spectrum was monitored on scan mode, the conformity of fragmentation between analytes and standard components was checked by selected ion monitoring mode (Table 2). Consequently,

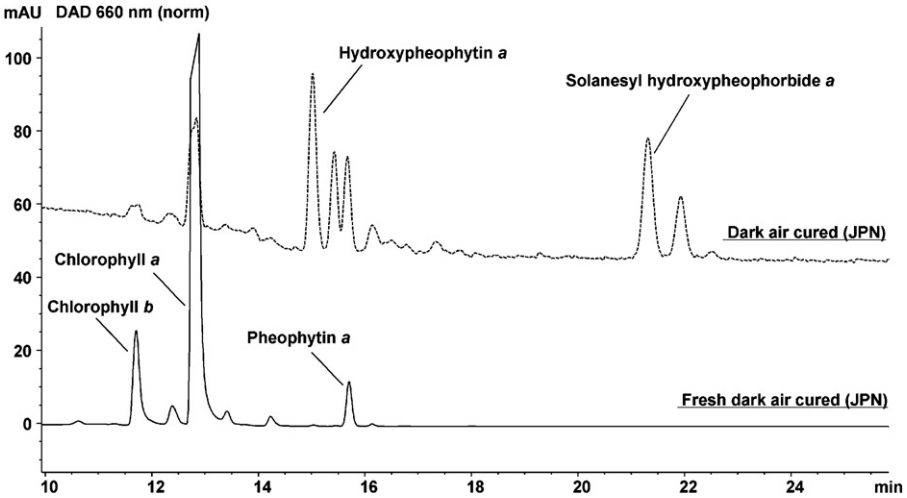

Fig. 9. Chromatograms of dark air-cured leaf and its fresh tobacco leaf using LC/DAD configured at 660 nm. The fresh leaf was cultivated in Japan, and then was treated with liquid nitrogen for pulverization. The following procedure was based on Sections 2.2 and 2.3.2.

the fragmentation of analytes showed the same spectrums as the standard components.

3.3. Origin of chlorophyll metabolites

Hydroxypheophytin *a*, *a*′, *b* and *b*′ (**5**, **6**, **9** and **10**) were first found in tobacco leaf. Considering the green color of the synthesized hydroxypheophytin *a* (**9**), such chlorophyll metabolite was considered to be related to the green color of Oriental leaf. The more interesting result from our research was that the solanesyl pheophorbide series (**16**, **17**, **20** and **21**) and the solanesyl hydroxypheophorbide series (**14**, **15**, **18** and **19**) were newly identified in tobacco leaf. The chlorophyll metabolites bound to solanesol in plants have not been reported yet. Meanwhile, tobacco leaves are known for including a large amount of solanesol [29–33] which is increasingly accumulated just before harvesting or during the curing process [14]. Therefore, they were considered tobacco specific components. However, since the origin and metabolic pathway of these components during the curing process remained unclear, a fresh tobacco leaf (dark air-cured leaf; usually dried in the similar way to burley) cultivated in Japan was analyzed to know whether the chlorophyll metabolites were included or not. Consequently, chlorophyll metabolites except for pheophytin *a* (**11**) was not detected (Fig. 9) in a fresh tobacco leaf. Chlorophyll *a* bound to solanesol instead of phytol was not detected, nor was hydroxychlorophyll *a*. These results indicated that the chlorophyll metabolites originate from pheophytin *a* (**11**) through oxidization or transesterification with solanesol during the curing process. It may be similarly feasible that solanesyl pheophytin *a* (**25**) and disolanesyl pheophorbide *a* (**28**) also derive from pheophytin *a*.

4. Conclusions

In this report, an expanded analytical method for the chlorophyll metabolites in Oriental tobacco leaf was developed. The wavelength spectrum, mass spectrum and retention time of each component using DAD and APCI/MSD made it possible to determine their detailed structures. Consequently, the identification of unknown chlorophyll metabolites was successfully accomplished. Some chlorophyll metabolites like hydroxypheophytin *a* and *b* were first found in tobacco leaves. More importantly, to our knowledge, solanesyl pheophorbide *a*, *b* and their hydroxylated components were first identified in plants. They might be tobacco specific components due to the large amount of solanesol in tobacco leaf. Given all investigations, they are derived from the pheophytin *a* through transesterification with solanesol. Since the expanded method made it possible to detect new other chlorophyll metabolites, it will be useful for searching for the other chlorophyll metabolites, knowing the specific characteristic of Oriental leaf and understanding the chemical change during the curing process.

Acknowledgement

The technical advice from Michinori Yokoi is gratefully acknowledged.

References

[1] J.M. Berg, J.L. Tymocako, L. Stryer (Eds.), Photosynthesis, Biochemistry, 4th edition, W.H. Freeman & Company, New York, 1995, p. 653.
[2] D. Dolphin, The Porphyrins Volume III Physical Chemistry Part A, Academic Press, New York, 1978.
[3] W.M. Manning, H.H. Strain, J. Biol. Chem. 151 (1943) 1.
[4] M. Chen, M. Schliep, R.D. Willows, Z. Cai, B.A. Neilan, H. Scheer, Science 329 (2010) 1318.
[5] G.R. Seely (Ed.), The Structure and Chemistry of Functional Groups, L.P. Vernon, The Chlorophylls, Academic Press, New York and London, 1966, p. 67.
[6] L. Almela, J.A. Fernández-López, M.J. Roca, J. Chromatogr. A 870 (2000) 483.
[7] K. Takamiya, T. Tsuchiya, H. Ohta, Trends Plant Sci. 5 (2000) 426.
[8] J.W. Heaton, A.G. Marangoni, Trends Food Sci. Technol. 7 (1996) 8.
[9] H. Thomas, H. Ougham, S. Hörtensteiner, Adv. Bot. Res. 35 (2001) 1.
[10] B. Kräutler, P. Matile, Acc. Chem. Res. 32 (1999) 35.
[11] S. Hörtensteiner, Cell. Mol. Life Sci. 56 (1999) 330.
[12] R.N. Jeffrey, R.B. Griffith, Plant Physiol. 22 (1) (1947) 34.
[13] H.R. Burton, M.J. Kasperbauer, J. Agric. Food Chem. 33 (1985) 879.
[14] J.C. Leffingwell, in: D. Davis, M.T. Nielsen (Eds.), Tobacco: Production Chemistry and Technology, Blackwell Science, Oxford, 1999, p. 265.
[15] Y. Suzuki, Y. Shioi, J. Agric. Food Chem. 51 (2003) 5307.
[16] P. Wongsinkongman, A. Brossi, H. Wang, K.F. Bastow, K. Lee, Bioorg. Med. Chem. 10 (2002) 583.
[17] L. Ma, D. Dolphin, J. Org. Chem. 61 (1996) 2501.
[18] A. Gauthier-Jacques, K. Bortlik, J. Hau, L.B. Fay, J. Agric. Food Chem. 49 (2001) 1117.
[19] S.C. Huang, C.F. Hung, W.B. Wu, B.H. Chen, J. Pharm. Biomed. Anal. 48 (2008) 105.
[20] R.L. Airs, J.E. Atkinson, B.J. Keely, J. Chromatogr. A 917 (2001) 167.
[21] N.A. Parris, J. Chromatogr. A 157 (1978) 161.
[22] D.J. Chitwood, G.W. Patterson, J. Liq. Chromatogr. Relat. Technol. 14 (1991) 151.
[23] P. Jandera1, G. Guiochon, J. Chromatogr. A 588 (1991) 1.
[24] V.M. Kapoulas, N.K. Andrikopoulos, J. Chromatogr. A 366 (1986) 311.
[25] E. Salivaras, A.R. McCurdy, J. Am. Oil Chem. Soc. 69 (1992) 935.
[26] J.S. Amaral, S.C. Cunha, M.R. Alves, J.A. Pereira, R.M. Seabra, B.P.P. Oliveira, J. Agric. Food Chem. 26 (2004) 7964.
[27] R.L. Rowland, P.H. Latimer, J.A. Giles, J. Am. Chem. Soc. 18 (1956) 4680.
[28] R.B.V. Breeman, F.L. Canjura, S.J. Schwartz, J. Agric. Food Chem. 39 (1991) 1452.
[29] Y. Zhao, Q. Du, J. Chromatogr. A 1151 (2007) 193.
[30] H. Zhou, C. Liu, J. Chromatogr. A 1129 (2006) 135.
[31] R.N. Rao, M.V.N.K. Talluri, T.S.V.N.M. Krishna, K. Ravindranath, J. Pharm. Biomed. Anal. 46 (2008) 310.
[32] C. Zhao, C. Li, Y. Zu, J. Pharm. Biomed. Anal. 44 (2007) 35.
[33] J. Chen, X. Liu, X. Xu, F.S. Lee, X. Wang, J. Pharm. Biomed. Anal. 43 (2007) 879.